nature astronomy

LETTERS

https://doi.org/10.1038/s41550-021-01458-1

Check for updates

Quiescent ultra-diffuse galaxies in the field originating from backsplash orbits

José A. Benavides[1,2]✉, Laura V. Sales[3], Mario. G. Abadi[1,2], Annalisa Pillepich[4], Dylan Nelson[5], Federico Marinacci[6], Michael Cooper[7], Ruediger Pakmor[8], Paul Torrey[9], Mark Vogelsberger[10] and Lars Hernquist[11]

Ultra-diffuse galaxies (UDGs) are the lowest-surface-brightness galaxies known, with typical stellar masses of dwarf galaxies but sizes similar to those of larger galaxies such as the Milky Way[1]. The reason for their extended sizes is debated, with suggested internal processes such as angular momentum[2], feedback[3,4] or mergers[5] versus external mechanisms[6–9] or a combination of both[10]. Observationally, we know that UDGs are red and quiescent in groups and clusters[11,12] whereas their counterparts in the field are blue and star-forming[13–16]. This dichotomy suggests environmental effects as the main culprits. However, this scenario is challenged by recent observations of isolated quiescent UDGs in the field[17–19]. Here we use the ΛCDM (or Λ cold dark matter, where Λ is the cosmological constant) cosmological hydrodynamical simulation to show that isolated quenched UDGs are formed as backsplash galaxies that were once satellites of another galactic, group or cluster halo but are today a few Mpc away from them. These interactions, albeit brief, remove the gas and tidally strip the outskirts of the dark matter haloes of the now quenched and seemingly isolated UDGs, which are born as star-forming field UDGs occupying dwarf-mass dark matter haloes. Quiescent UDGs may therefore be found in non-negligible numbers in filaments and voids, bearing the mark of past interactions as stripped outer haloes devoid of dark matter and gas compared to dwarfs with similar stellar content.

Ultra-diffuse galaxies (UDGs) in groups and clusters are characterized by a puzzling wide range of dark matter and globular cluster content[20–22], thick disk-like shapes[11,23], old stellar populations[24] and no substantial gas component. Their quiescence is not surprising given the high-density environments they populate. However, for the few quenched UDGs that have been discovered in the field, the mechanism responsible for removing the gas and halting star formation remains unknown. On the theory side, progress requires high-resolution cosmological simulations that are able to resolve the myriad of environments and physics involved in this problem, from the formation of isolated dwarfs in their haloes to their interactions with filaments, groups and clusters. Such simulations have only recently become possible, with the TNG50 simulation (used here) among those with the highest resolution available[25,26].

We use the stellar mass–size relation defined by all simulated galaxies (Fig. 1, grey dots) to define our sample of field UDGs as those central galaxies (excluding satellites) with stellar mass in the dwarf range ($\log(M_\star/M_\odot)=[7.5,9]$, shaded pink region) and a stellar size above the 95th percentile at a given mass (magenta stars). Our definition overlaps with observational samples of UDGs[14,18,27,28]. We study the origin of the extended sizes of these galaxies elsewhere (J.A.B. et al., manuscript in preparation) but a brief summary is given in Supplementary Fig. 2.

Galaxy colours ($g-r$) of our simulated UDGs in Fig. 2 show a clear bimodality: most central UDGs are in the 'blue cloud', suggesting young stellar populations as expected for dwarfs in the field, whereas 23.7% of our simulated UDGs are along the red sequence. The mass distribution is non-uniform, with red UDGs being more common towards the lower masses, where also, at the same mass, field UDGs have a higher fraction of red objects than normal dwarfs in the field (Supplementary Fig. 2, upper panel). Their colours correlate with their star formation rates (SFRs) (Fig. 2, inset), with the blue UDGs occupying the 'main sequence' of star-forming galaxies and the red UDGs showing negligible star formation today.

A close inspection of the histories of our red quiescent UDGs reveals a factor in common: they have all been satellites of another system in the past but are today central galaxies in the field. An example of the orbit of one of our red UDGs is shown in Fig. 3a. This dwarf interacted ~4 billion years ago with a group that has a virial mass $M_{200}(z=0)\approx 6.46\times10^{13}\,M_\odot$ but is found today ~1.5 Mpc away, more than twice the virial radius of the group. (Virial quantities refer to the radius enclosing 200 times the critical density of the Universe.) The colour coding of the orbit, reflective of the dwarf colour at each time, shows that the reddening starts already as it falls into the group and accelerates after the pericentric passage. The images of the simulated UDG (Fig. 3b) clearly show that its gas is removed as it approaches the pericentre, explaining its quiescence and redness today in the field. The stellar size is not largely affected by the interaction; our red UDGs were all already extended before infall (Supplementary Fig. 1).

Objects in such external orbits, which are found far beyond the virial radius of their hosts, are known as backsplash galaxies[29] and are a natural consequence of the hierarchical assembly in ΛCDM. Our red UDGs are backsplash objects of systems in a wide range

[1]Instituto de Astronomía Teórica y Experimental, CONICET-UNC, Córdoba, Argentina. [2]Observatorio Astronómico de Córdoba, Universidad Nacional de Córdoba, Córdoba, Argentina. [3]Department of Physics and Astronomy, University of California, Riverside, CA, USA. [4]Max-Planck-Institut für Astronomie, Heidelberg, Germany. [5]Institut für Theoretische Astrophysik, Zentrum für Astronomie, Universität Heidelberg, Heidelberg, Germany. [6]Department of Physics and Astronomy 'Augusto Righi', University of Bologna, Bologna, Italy. [7]Department of Physics and Astronomy, University of California, Irvine, CA, USA. [8]Max-Planck-Institut für Astrophysik, Garching, Germany. [9]Department of Astronomy, University of Florida, Gainesville, FL, USA. [10]Department of Physics, Massachusetts Institute of Technology, Cambridge, MA, USA. [11]Institute for Theory and Computation, Harvard-Smithsonian Center for Astrophysics, Cambridge, MA, USA. ✉e-mail: jose.benavides@unc.edu.ar

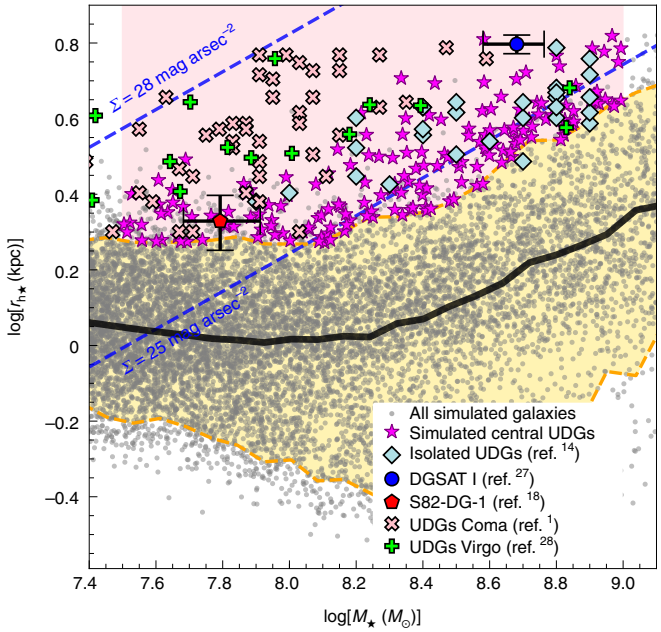

Fig. 1 | Definition of the UDG sample. Stellar mass versus size ($M_\star$ versus $r_{h\star}$) relation for all simulated galaxies in the mass range $\log(M_\star/M_\odot)=[7.4, 9.1]$ in the TNG50 simulation (grey dots). Thin blue dashed curves indicate lines of constant surface brightness assuming a mass-to-light ratio equal to 1. The solid black line indicates the median size at fixed $M_\star$ for the simulated galaxies. Yellow dashed curves show the 5th and 95th percentiles, with the shaded yellow region in between highlighting the sample of normal galaxies. Our sample of field UDGs (magenta stars) is defined as central galaxies with $\log(M_\star/M_\odot)=[7.5, 9]$ and stellar size above the 95th percentile (pink shaded region). Several observational data are shown in black-edged symbols, where we transform two-dimensional sizes $R_{\rm eff}$ to three-dimensional assuming $r_{h\star}=4/3\,R_{\rm eff}$. Light blue diamonds indicate star-forming UDGs in low-density environments[14], the dark blue circle is the relatively isolated DGSAT I (ref. [27]) and the red pentagon is UDG S82-DG-1, an isolated quiescent UDG[18]. For comparison, we also show UDGs in the Virgo cluster[28] (green crosses) and the Coma cluster[1] (pink X symbols). Our UDG definition agrees well with observational samples, in particular for those in low-density environments.

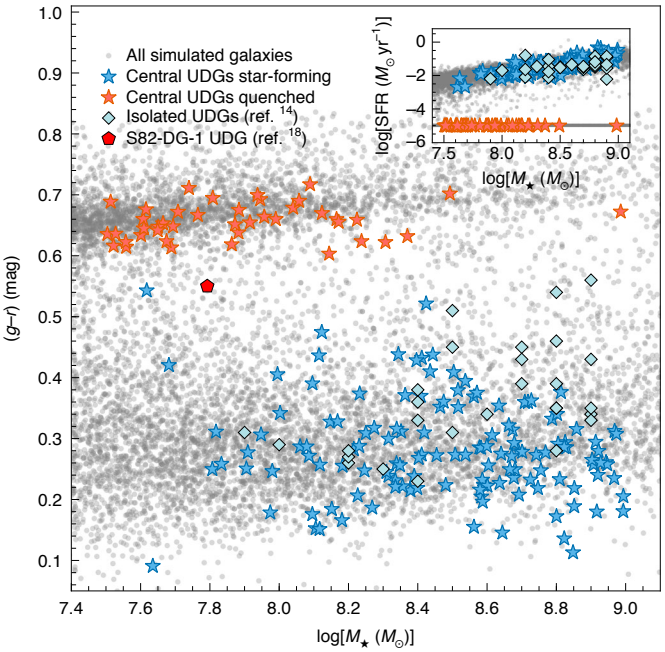

Fig. 2 | Dichotomy in colour and star formation rate of field UDGs. Colour $(g-r)$ as a function of stellar mass for all simulated galaxies in this mass range (grey dots) and field UDGs (starred symbols). Most field UDGs are blue, but about a quarter of the sample populates the 'red sequence'. These colours correlate with SFRs (inset), where blue UDGs are star-forming and red UDGs are quiescent (SFR is zero in these objects but has been artificially shifted to $10^{-5}\,M_\odot\,{\rm yr}^{-1}$ for plotting purposes). Coloured symbols correspond to available observational data: isolated star-forming UDGs[14] with light blue diamonds and S82-DG-1 (ref. [18]) with red pentagons.

of virial masses, from galaxy-sized haloes with $M_{200}\approx 2\times10^{12}\,M_\odot$ to galaxy clusters, and are today on average at $2.1\,r_{200}$ from those systems, or 1.7 ± 0.7 Mpc, but can reach as far as 3.35 Mpc in some cases (Supplementary Fig. 3). In the large majority of cases (64.3%), the system responsible for the quenching and the launching beyond the virial radius is the same, with the remaining cases being 'pre-processing', meaning that the UDG was first quenched in a moderate mass host, which subsequently fell into a more massive system responsible for the energetic orbit.

A section of the simulated box with the location of red and blue UDGs is illustrated in Fig. 3c, highlighting the red UDGs that are backsplash objects of galaxy-size haloes (green circles), located mainly in low-density regions of the Universe. Red field UDGs cluster more than the blue ones, but they are all at substantial distances from their once-hosts. On average, the interactions occurred 5.5 ± 2.5 Gyr ago and were moderately quick, with red UDGs spending typically 1.5 Gyr (median) within the virial radius of the systems they are backsplash of (Supplementary Fig. 4).

Interestingly, there are extreme cases in which the close pericentre passage of the UDG results in its total ejection from the system in a way that is reminiscent of those in multiple-body interactions[30]. Our most extreme UDG resides ~3.35 Mpc away from its host and would appear as an extremely isolated object in a void-like environment (Fig. 3c, yellow circle). This UDG fell in as part of a galaxy-size group into a group-size halo with $M_{200}(z=0)=3.36\times10^{13}\,M_\odot$ and was ejected more than 6 Gyr ago after its first pericentre (Supplementary Fig. 5).

This scenario for the formation of quiescent UDGs in the field has a number of observational implications. First, the stellar populations are old due to the quenching during the backsplash interaction. As shown in Fig. 4a, blue UDGs are comparatively younger, characterized by an extended star formation history as argued in the case of observed field UDGs[15], and consistent with the overall simulated population of field dwarfs (grey symbol). Note that the ages inferred for isolated UDGs in observations are mostly in agreement with our blue UDG population.

Second, the morphologies of red UDGs are always more spheroid-dominated than their blue counterparts with similar stellar mass, which might show spheroid or disk structure (Fig. 4b), in agreement with previous work[31]. Here, morphology is quantified by the $\kappa_{\rm rot}$ parameter (Methods). We predict a shift towards early-type morphologies for red UDGs (low $\kappa_{\rm rot}$), which is consistent with the picture in which satellite galaxies are preferentially spheroid-dominated due to transformations induced by the environment[32].

Third and most important, backsplash galaxies have been stripped to some degree of their mass during the tidal interaction with their past host system. Blue UDGs form in dwarf-mass haloes with virial mass in the range $\log(M_{200}/M_\odot)=[10.3–11.2]$, whereas red UDGs at the same stellar mass show lower virial masses, with a median of $\log(M_{200}/M_\odot)=9.73$ (Fig. 4c) due to this interaction. Red UDGs in the field should be clear outliers compared to predictions

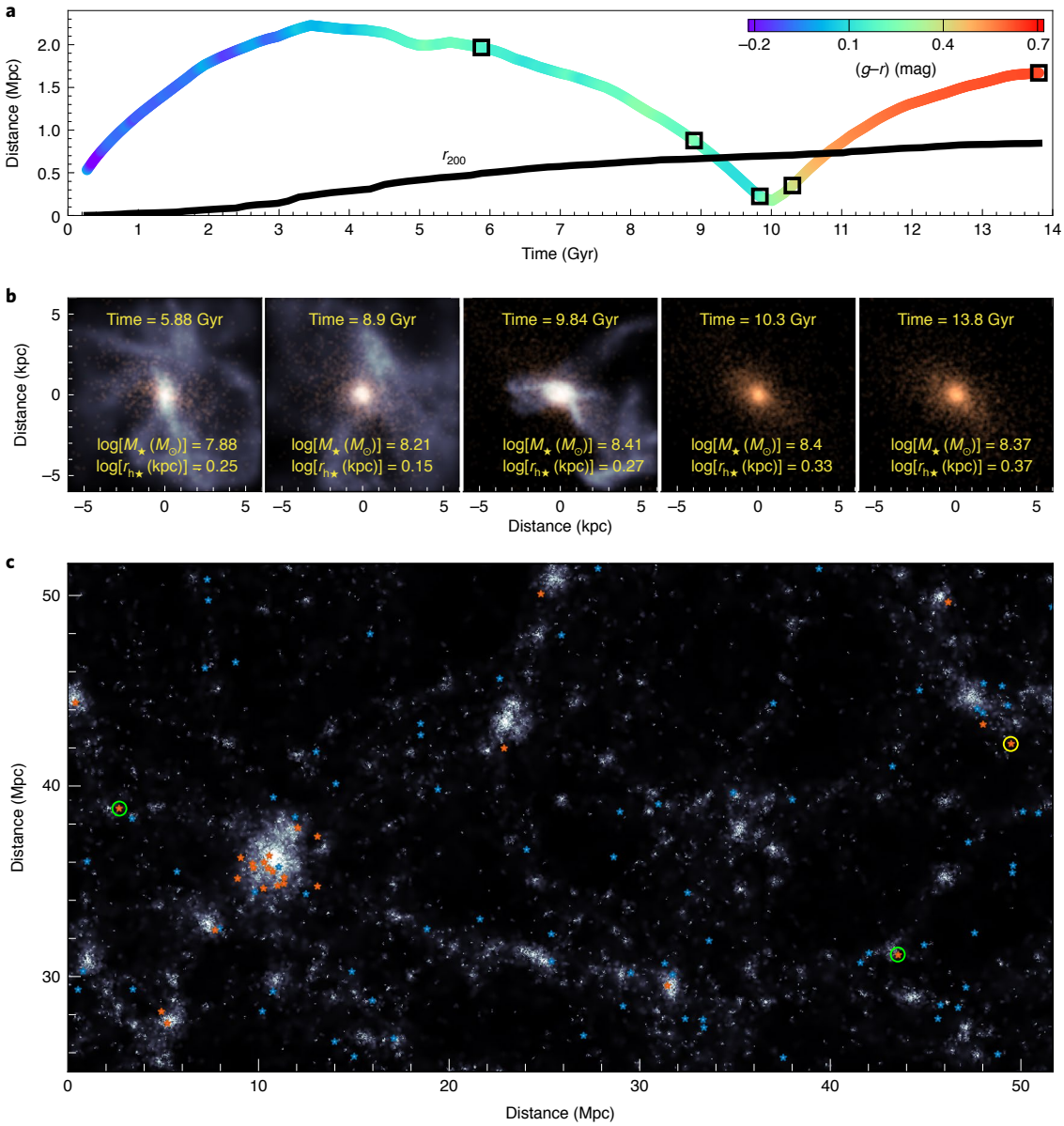

Fig. 3 | Formation of red UDGs in backsplash orbits and their location in the Universe. a, Example orbit of one of our quiescent UDGs around its temporary (group-size) host halo, whose virial radius is indicated by the black line. The orbit is colour-coded according to the instantaneous (g−r) colour in the dwarf (see colour bar at top right) and shows that reddening starts right after pericentre. **b**, Snapshot view of the stellar (red) and gas (blue) content of the UDG in different epochs along its orbit (times are highlighted by the black squares in **a**). The gas is fully removed while approaching the pericentre, resulting in posterior aging and reddening of the stellar population. **c**, Location of blue and red UDGs (starred symbols) in part of the simulation box. Structure is shown in the grey map as traced by all galaxies in the halo catalogue. Red UDGs are spatially more clustered than blue ones, but some might exist even in regions of very low density. For instance, the open green circles correspond to UDGs that are backsplash objects of galactic haloes with $\log(M_{200}/M_\odot) \approx 12.5$. The single yellow circle indicates the most extreme case of an ejected UDG located ~3.35 Mpc from its host.

from abundance-matching models[33]. The stripping occurs mostly in the outer halo, where the dark matter density profile of red UDGs falls more steeply than that of the unperturbed blue UDG population (Supplementary Fig. 6). Unfortunately, the inner stellar velocity dispersion of red and blue UDGs—a possible observable—is statistically indistinguishable in our simulation.

A fourth implication in this scenario is that red UDGs are fully devoid of halo gas, which was all removed via ram pressure[34,35] along with the inner gas during the interaction with their hosts. We have checked that no gas is re-accreted in these dwarfs, in contrast with the gas mass $M_{gas} = 10^8$ to $10^{10} M_\odot$ predicted in the haloes of blue UDGs in the field (this includes gas with distance (in kpc) of $2r_{h\star} < r < r_{200}$, where $r_{h\star}$ is the stellar half-mass radius). A promising way to study the circumgalactic medium of these galaxies down to very low column densities is to use background quasars to provide different absorption lines-of-sight across a halo[36]. Although this would be prohibitive on an individual UDG basis, a statistical detection (or lack of thereof) might be achieved once a sufficiently large number of red field UDGs are found. Neutral gas and Hα studies of red UDGs should also confirm a lack of gas in their interstellar medium.

There are a few observational detections of quiescent UDGs in low-density environments and they seem consistent with the picture emerging from our analysis. One of the first reported non-cluster

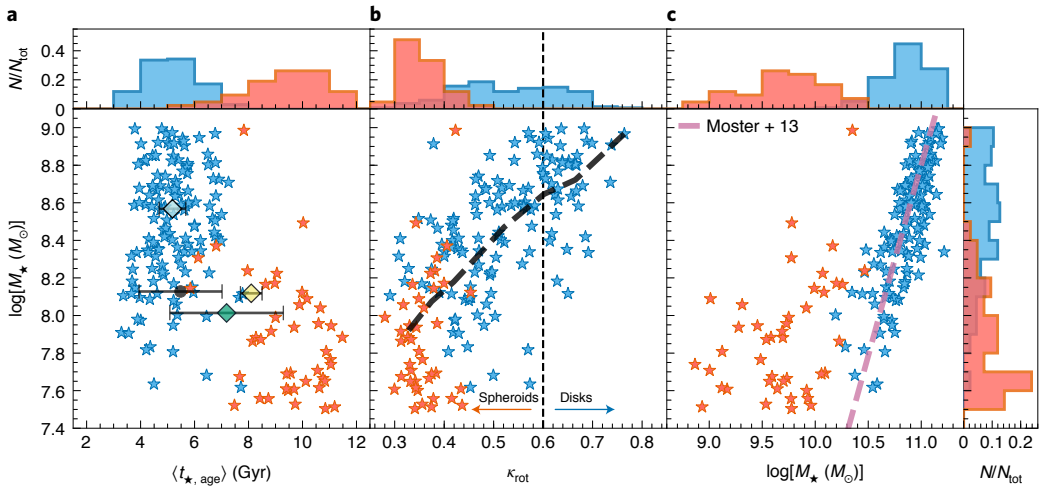

Fig. 4 | Predicted properties of field red versus blue UDGs. a, Average age of the population (mass-weighted) as a function of stellar mass. Red UDGs are older than the blue UDGs (averages for red and blue are 5.21 ± 0.99 Gyr and 9.40 ± 1.38 Gyr, respectively). Blue UDGs have ages consistent with the overall sample of simulated normal (non-UDG) field dwarfs in the same mass range, as shown by the grey symbol with error bars corresponding to 5th to 95th percentiles. Available observational data are shown for comparison: star-forming UDGs[14] with light blue diamond, DGSAT I (ref. [27]) with yellow diamond and average of UDGs in the Coma cluster[24] with green diamond. **b**, Morphology quantified by the parameter κ_{rot}, where $\kappa_{rot} > 0.6$ (indicated by the vertical thin dashed line) highlights disk-dominated objects (Methods). Red UDGs have typically more spheroidal morphology (lower κ_{rot} values) than the blue population at similar mass. The thick black dashed curve shows the median κ_{rot} at a given stellar mass. **c**, Virial mass (M_{200}) versus stellar mass relation. Red UDGs have stripped outer haloes and show today lower virial masses at fixed stellar mass. The pink dashed curve corresponds to the abundance-matching model by ref. [33]. Histograms, showing normalized numbers (N/N_{tot}) of UDGs, along all axes are included to ease the comparisons.

UDGs is DGSAT I (ref. [17]), which is located in the filament of the Pisces-Perseus supercluster. This is in excellent agreement with our predictions, which show that most red field UDGs are nearby but outside groups and clusters. DGSAT I lacks gas (as measured by Hα (ref. [17])) and has a relatively old stellar population (8.1 ± 0.4 Gyr mass-weighted age[27]), which is also within the range predicted by our simulations.

Another interesting object is S82-DG-1, an extremely isolated quenched UDG in a nearby void[18]. Its isolation has been used to favour internal effects such as feedback to explain the possible origin of UDGs, rather than high-density environmental effects. Here, we argue that S82-DG-1 fits the characteristic expected for our simulated population of passive UDGs that were satellites of a galactic-size host. S82-DG-1 is located at ~55 kpc in projection and at a redshift distance of less than $\Delta v = 145\,\mathrm{km\,s^{-1}}$ from NGC 1211, a lenticular galaxy with stellar mass $M_\star \approx 1 \times 10^{10}\,M_\odot$ (Methods). Three of our simulated red UDGs have been backsplash objects in galaxy-mass haloes $M_{200} < 10^{13}\,M_\odot$ and are found today ~650 kpc from their hosts. Moreover, 12 red isolated UDGs (28.5%) were quenched in galactic environments ($M_{200} < 10^{13}\,M_\odot$). Although the exact distance of S82-DG-1 to NGC 1211 is unknown, our analysis provides support for the possible external nature of quenching in S82-DG-1 induced by NGC 1211. The old stellar population inferred for S82-DG-1, 6 Gyr of age[18], is in excellent agreement with the average time of the interactions found in our simulated sample.

We therefore propose backsplash orbits as a new mechanism to explain the presence of quiescent UDGs in low-density environments. This population of red and diffuse dwarfs results from the infall of normal star-forming field UDGs into galactic, group or cluster-size haloes responsible for stripping off their gas and propelling them to distances ~1 Mpc and beyond. In the most extreme cases, UDGs may even be ejected several Mpc away from these systems. The predicted fraction of red UDGs in our simulation in the studied mass range is ~24%. Mild clustering and old stellar populations, along with dark matter haloes of lower mass and the complete absence of gas in the galactic and circumgalactic region, are the expected telltales of this formation scenario for red UDGs. Future wide-field surveys targeting the surrounding of groups and clusters may be the most promising way to uncover this population of elusive dwarfs predicted as a natural consequence of the assembly of haloes in ΛCDM.

Methods

Simulation data and property determination. For our calculations, we use the cosmological hydrodynamical TNG50 simulation[25,26] of the IllustrisTNG project[37–43]. The IllustrisTNG galaxy formation model presents improvements in physics due to the effects of active galactic nuclei and feedback[37,44] compared to the original Illustris, its predecessor[45–47]. The simulation was run using the moving-mesh code AREPO[48,49]. Besides gravity, the runs model a set of physical processes relevant to galaxy formation including gas cooling and heating, star formation, metal enrichment, stellar and black hole feedback and magnetic fields.

The simulation is initialized at redshift $z = 127$ using the N-GENIC code[50] with cosmological parameters consistent with the Planck mission results[51]: $\Omega_m = \Omega_{DM} + \Omega_b = 0.3089$, $\Omega_b = 0.0486$, cosmological constant $\Omega_\Lambda = 0.6911$, Hubble constant $H_0 = 100\,h\,\mathrm{km\,s^{-1}\,Mpc^{-1}}$ (with $h = 0.6774$), $\sigma_8 = 0.8159$ and spectral index $n_s = 0.9667$, where Ω is the cosmic density parameter, σ_8 is the fluctuation amplitude at $8\,\mathrm{Mpc\,h^{-1}}$, and the subscript m refers to total matter (dark matter, DM, plus baryons, b).

TNG50 is the smallest box from the TNG suite (50.7 Mpc (comoving) on a side compared to 100 Mpc and 300 Mpc) but the one with the highest resolution; a total of $2{,}160^3$ gas and dark matter particles are set in the initial conditions, resulting in a mass per particle $m_{bar} = 8.4 \times 10^4\,M_\odot$ and $m_{DM} = 4.6 \times 10^5\,M_\odot$ for the baryons and dark matter, respectively. The gravitational softening for the stars and dark matter is 0.29 kpc (comoving), whereas the gas has adaptive softening down to 74 pc (physical). TNG50 is the only simulation of its kind and resolution that is able to follow such a wide range of environments from dwarf haloes to clusters of galaxies. The TNG50 box includes one halo with $\log(M_{200}/M_\odot) > 14$ and a substantial number of less massive haloes ($13 < \log(M_{200}/M_\odot) < 14$), which allows the analysis of galaxies in the high-density environments of groups and clusters.

The identification of groups is done via the friends-of-friends (FoF)[52] algorithm followed by SUBFIND to identify substructure[53]. Subhaloes containing a stellar component are considered galaxies. Galaxies are classified either as 'centrals' (main galaxy in each group) or 'satellites' otherwise. Here we use centrals to identify the population of dwarf galaxies in the field, meaning they are not satellites of any more massive system. Galaxy quantities such as stellar mass $M_\star$, morphology, age and star formation rate are defined using particles within the 'galactic radius', which is defined as twice the half-mass radius of the stars: $r_{gal} = 2\,r_{h\star}$. Luminosities (used to compute colours) correspond to all stellar particles assigned to the galaxy (field SubhaloStellarPhotometrics in the halo catalogue[54]).

The morphology parameter κ_{rot} is calculated following ref. [55] as follows. After rotating each galaxy to a reference frame where the angular momentum of the stars (within r_{gal}) points along the z direction, we compare the energy in rotation around the z axis to the total kinetic energy K as $\kappa_{rot} = (1/K)\,\Sigma\,(1/2mj_z^2/R)$, where j_z is the angular momentum of each stellar particle in the rotated system, m is their mass and R is their cylindrical radius, and the sum is over stars within r_{gal}. Defined in this way, the morphology parameter κ_{rot} has been shown to correlate with other definitions of galaxy morphology[55,56]. Low κ_{rot} values correspond to spheroid-dominated objects, whereas $\kappa_{rot} > 0.6$ is used to identify disk-dominated objects.

Galaxies are followed over time by means of Sublink merger trees[57]. This allows us to track the mass, size and star formation histories of our sample over time. Note that the circumgalactic gas properties in galactic-size and group-size haloes in TNG50 are in good agreement with observational constraints[26,58] and may therefore provide a solid theoretical ground to study environmental effects in our UDG sample.

The stellar mass for the lenticular galaxy NGC 1211 was estimated from its V-band luminosity in ref. [59] and assuming a mass-to-light ratio of 1 for simplicity.

Sample of field UDGs. The criterion to define UDGs varies across different works in the literature. Here we define UDGs as the most extended outliers of the stellar mass–size relation, following the philosophy introduced in ref. [28]. The galaxy modelling used in the TNG100 and TNG50 simulations has been shown to agree well with observational constraints on the stellar mass–size relation of the galaxy population[25,60]. In this work, we construct the mass–size relation using well-resolved galaxies, defined as those with dark matter mass $m_{DM} \geq 5\times10^7\,M_\odot$ (with total dark matter mass assigned by SUBFIND to each subhalo), stellar mass $m_\star \geq 5\times10^6\,M_\odot$ and size $r_{h\star} \geq 0.3$ kpc; this results in a minimum number of ~60 stellar particles and 110 dark matter particles.

Figure 1 shows the stellar mass–size relation, where the median at fixed $M_\star$ is indicated by the thick black line. We notice that for $\log(M_\star/M_\odot) < 7.5$ the median starts to steadily increase towards lower-mass objects, an effect not found in observation and of origin likely numerical. To be conservative, we study only dwarf galaxies in the stellar mass range $\log(M_\star/M_\odot) = [7.5, 9]$. More than 8,600 dwarf galaxies in TNG50 satisfy this mass cut. The distribution of sizes at a given stellar mass is approximately log-normal. We therefore select the 5% most extended outliers at fixed $M_\star$ as our UDG population, deeming all galaxies within the 5th to 95th percentile range to be 'normal' galaxies. This results in an average half-mass radius of 2.5 ± 0.8 kpc for our UDG population. From the UDGs identified in this way, 176 are centrals to their haloes (or 'field' population) and constitute the sample analysed here (the study of UDGs as satellites is presented elsewhere by J.A.B. et al., manuscript in preparation). Figure 1 shows that our definition for UDG galaxies is in very good agreement with several observational samples of star-forming and quenched UDGs in low-density environments[14,18,27].

Visualizations. Images shown in Fig. 3 were made using the Py-SPHViewer code[61] v1.0.0. This code smooths the particle information into two-dimensional histograms to reflect the underlying continuous density field. For the specific case of the small panels in Fig. 3b, we combined the information from the gas cells (blue hues) and the stellar particles (red). Each stamp has 150×150 pixels, and we use 12 neighbours for the smoothing. We use all gas or stellar particles identified to belong to this subhalo by SUBFIND that are within the image box (12 kpc (physical) on a side). For Fig. 3c, we use the x and y coordinates of each subhalo in the halo catalogue. The image is smoothed using a three-neighbour kernel density estimation and has $1{,}000\times500$ pixels.

Data availability

This letter is based on snapshots, subhalo catalogues and merger trees from the cosmological hydrodynamical TNG50 simulation[25,26] of the IllustrisTNG project[37–43]. These data are publicly available at https://www.tng-project.org/. ASCII tables with the simulation data for our sample of UDGs in Figs. 1, 2 and 4 are available in the public repository https://github.com/josegit88/public_data_files/tree/main/ascii_files_isolated_UDGs_TNG50. Source data are provided with this paper.

Code Availability

Scripts used for reading of and access to the snapshot, merger trees and subhalo data are publically available at the TNG database. Visualizations were made using the publicly available Py-SPHViewer code[61]. Any correspondence and/or request for materials pertaining to this manuscript should be directed to J.A.B.

Received: 4 March 2021; Accepted: 20 July 2021;
Published online: 6 September 2021

References

1. van Dokkum, P. G. et al. Forty-seven Milky Way-sized, extremely diffuse galaxies in the Coma cluster. *Astrophys. J. Lett.* **798**, L45 (2015).
2. Amorisco, N. C. & Loeb, A. Ultradiffuse galaxies: the high-spin tail of the abundant dwarf galaxy population. *Mon. Not. R. Astron. Soc.* **459**, L51–L55 (2016).
3. Di Cintio, A. et al. NIHAO – XI. Formation of ultra-diffuse galaxies by outflows. *Mon. Not. R. Astron. Soc.* **466**, L1–L6 (2017).
4. Chan, T. K. et al. The origin of ultra diffuse galaxies: stellar feedback and quenching. *Mon. Not. R. Astron. Soc.* **478**, 906–925 (2018).
5. Wright, A. C. et al. The formation of isolated ultradiffuse galaxies in ROMULUS25. *Mon. Not. R. Astron. Soc.* **502**, 5370–5389 (2021).
6. Safarzadeh, M. & Scannapieco, E. The fate of gas-rich satellites in clusters. *Astrophys. J.* **850**, 99 (2017).
7. Carleton, T. et al. The formation of ultra-diffuse galaxies in cored dark matter haloes through tidal stripping and heating. *Mon. Not. R. Astron. Soc.* **485**, 382–395 (2019).
8. Jiang, F. et al. Formation of ultra-diffuse galaxies in the field and in galaxy groups. *Mon. Not. R. Astron. Soc.* **487**, 5272–5290 (2019).
9. Tremmel, M. et al. The formation of ultradiffuse galaxies in the RomulusC galaxy cluster simulation. *Mon. Not. R. Astron. Soc.* **497**, 2786–2810 (2020).
10. Sales, L. V. et al. The formation of ultradiffuse galaxies in clusters. *Mon. Not. R. Astron. Soc.* **494**, 1848–1858 (2020).
11. Koda, J., Yagi, M., Yamanoi, H. & Komiyama, Y. Approximately a thousand ultra-diffuse galaxies in the Coma cluster. *Astrophys. J. Lett.* **807**, L2 (2015).
12. Yagi, M., Koda, J., Komiyama, Y. & Yamanoi, H. Catalog of ultra-diffuse galaxies in the Coma clusters from Subaru imaging data. *Astrophys. J. Suppl. Ser.* **225**, 11 (2016).
13. Greco, J. P. et al. A study of two diffuse dwarf galaxies in the field. *Astrophys. J.* **866**, 112 (2018).
14. Rong, Y. et al. Lessons on star-forming ultra-diffuse galaxies from the stacked spectra of the Sloan Digital Sky Survey. *Astrophys. J. Lett.* **899**, L12 (2020).
15. Barbosa, C. E. et al. One Hundred SMUDGes in S-PLUS: ultra-diffuse galaxies glourish in the field. *Astrophys. J. Suppl. Ser.* **247**, 46 (2020).
16. Tanoglidis, D. et al. Shadows in the dark: low-surface-brightness galaxies discovered in the Dark Energy Survey. *Astrophys. J. Suppl. Ser.* **252**, 18 (2021).
17. Martínez-Delgado, D. et al. Discovery of an ultra-diffuse galaxy in the Pisces-Perseus supercluster. *Astron. J.* **151**, 96 (2016).
18. Román, J., Beasley, M. A., Ruiz-Lara, T. & Valls-Gabaud, D. Discovery of a red ultra-diffuse galaxy in a nearby void based on its globular cluster luminosity function. *Mon. Not. R. Astron. Soc.* **486**, 823–835 (2019).
19. Prole, D. J., van der Burg, R. F. J., Hilker, M. & Spitler, L. R. The quiescent fraction of isolated low surface brightness galaxies: observational constraints. *Mon. Not. R. Astron. Soc.* **500**, 2049–2062 (2021).
20. van Dokkum, P. et al. A galaxy lacking dark matter. *Nature* **555**, 629–632 (2018).
21. Lim, S. et al. The globular cluster systems of ultra-diffuse galaxies in the Coma cluster. *Astrophys. J.* **862**, 82 (2018).
22. Doppel, J. E. et al. Globular clusters as tracers of the dark matter content of dwarfs in galaxy clusters. *Mon. Not. R. Astron. Soc.* **502**, 1661–1677 (2021).
23. Mancera Piña, P. E. et al. The evolution of ultra-diffuse galaxies in nearby galaxy clusters from the Kapteyn IAC WEAVE INT Clusters Survey. *Mon. Not. R. Astron. Soc.* **485**, 1036–1052 (2019).
24. Ferré-Mateu, A. et al. Origins of ultradiffuse galaxies in the Coma cluster – II. Constraints from their stellar populations. *Mon. Not. R. Astron. Soc.* **479**, 4891–4906 (2018).
25. Pillepich, A. et al. First results from the TNG50 simulation: the evolution of stellar and gaseous discs across cosmic time. *Mon. Not. R. Astron. Soc.* **490**, 3196–3233 (2019).
26. Nelson, D. et al. First results from the TNG50 simulation: galactic outflows driven by supernovae and black hole feedback. *Mon. Not. R. Astron. Soc.* **490**, 3234–3261 (2019).
27. Martín-Navarro, I. et al. Extreme chemical abundance ratio suggesting an exotic origin for an ultradiffuse galaxy. *Mon. Not. R. Astron. Soc.* **484**, 3425–3433 (2019).
28. Lim, S. et al. The Next Generation Virgo Cluster Survey (NGVS). XXX. Ultra-diffuse galaxies and their globular cluster systems. *Astrophys. J.* **899**, 69 (2020).
29. Balogh, M. L., Navarro, J. F. & Morris, S. L. The origin of star formation gradients in rich galaxy clusters. *Astrophys. J.* **540**, 113–121 (2000).
30. Sales, L. V., Navarro, J. F., Abadi, M. G. & Steinmetz, M. Cosmic ménage à trois: the origin of satellite galaxies on extreme orbits. *Mon. Not. R. Astron. Soc.* **379**, 1475–1483 (2007).
31. Cardona-Barrero, S. et al. NIHAO XXIV: rotation- or pressure-supported systems? Simulated ultra diffuse galaxies show a broad distribution in their stellar kinematics. *Mon. Not. R. Astron. Soc.* **497**, 4282–4292 (2020).
32. Joshi, G. D. et al. The fate of disc galaxies in IllustrisTNG clusters. *Mon. Not. R. Astron. Soc.* **496**, 2673–2703 (2020).
33. Moster, B. P., Naab, T. & White, S. D. M. Galactic star formation and accretion histories from matching galaxies to dark matter haloes. *Mon. Not. R. Astron. Soc.* **428**, 3121–3138 (2013).

34. Gunn, J. E. & Gott, J. R.III On the infall of matter into clusters of galaxies and some effects on their evolution. *Astrophys. J.* **176**, 1–19 (1972).
35. Abadi, M. G., Moore, B. & Bower, R. G. Ram pressure stripping of spiral galaxies in clusters. *Mon. Not. R. Astron. Soc.* **308**, 947–954 (1999).
36. Tumlinson, J., Peeples, M. S. & Werk, J. K. The circumgalactic medium. *Annu. Rev. Astron. Astrophys.* **55**, 389–432 (2017).
37. Pillepich, A. et al. Simulating galaxy formation with the IllustrisTNG model. *Mon. Not. R. Astron. Soc.* **473**, 4077–4106 (2018).
38. Pillepich, A. et al. First results from the IllustrisTNG simulations: the stellar mass content of groups and clusters of galaxies. *Mon. Not. R. Astron. Soc.* **475**, 648–675 (2018).
39. Springel, V. et al. First results from the IllustrisTNG simulations: matter and galaxy clustering. *Mon. Not. R. Astron. Soc.* **475**, 676–698 (2018).
40. Nelson, D. et al. First results from the IllustrisTNG simulations: the galaxy colour bimodality. *Mon. Not. R. Astron. Soc.* **475**, 624–647 (2018).
41. Naiman, J. P. et al. First results from the IllustrisTNG simulations: a tale of two elements – chemical evolution of magnesium and europium. *Mon. Not. R. Astron. Soc.* **477**, 1206–1224 (2018).
42. Marinacci, F. et al. First results from the IllustrisTNG simulations: radio haloes and magnetic fields. *Mon. Not. R. Astron. Soc.* **480**, 5113–5139 (2018).
43. Nelson, D. et al. The IllustrisTNG simulations: public data release. *Comput. Astrophys. Cosmol.* **6**, 2 (2019).
44. Weinberger, R. et al. Simulating galaxy formation with black hole driven thermal and kinetic feedback. *Mon. Not. R. Astron. Soc.* **465**, 3291–3308 (2017).
45. Vogelsberger, M. et al. Introducing the Illustris Project: simulating the coevolution of dark and visible matter in the Universe. *Mon. Not. R. Astron. Soc.* **444**, 1518–1547 (2014).
46. Vogelsberger, M. et al. Properties of galaxies reproduced by a hydrodynamic simulation. *Nature* **509**, 177–182 (2014).
47. Genel, S. et al. Introducing the Illustris project: the evolution of galaxy populations across cosmic time. *Mon. Not. R. Astron. Soc.* **445**, 175–200 (2014).
48. Springel, V. E pur si muove: Galilean-invariant cosmological hydrodynamical simulations on a moving mesh. *Mon. Not. R. Astron. Soc.* **401**, 791–851 (2010).
49. Weinberger, R., Springel, V. & Pakmor, R. The AREPO public code release. *Astrophys. J. Suppl. Ser.* **248**, 32 (2020).
50. Springel, V. N-GenIC: cosmological structure initial conditions *Astrophysics Source Code Library* ascl: 1502.003 (2015).
51. Alves, J., Combes, F., Ferrara, A., Forveille, T. & Shore, S. Planck 2015 results. *Astron. Astrophys.* **594**, E1 (2016).
52. Davis, M., Efstathiou, G., Frenk, C. S. & White, S. D. M. The evolution of large-scale structure in a universe dominated by cold dark matter. *Astrophys. J.* **292**, 371–394 (1985).
53. Springel, V., White, S. D. M., Tormen, G. & Kauffmann, G. Populating a cluster of galaxies – I. Results at $z=0$. *Mon. Not. R. Astron. Soc.* **328**, 726–750 (2001).
54. Nelson, D. et al. The Illustris simulation: public data release. *Astron. Comput.* **13**, 12–37 (2015).
55. Sales, L. V. et al. The origin of discs and spheroids in simulated galaxies. *Mon. Not. R. Astron. Soc.* **423**, 1544–1555 (2012).
56. Snyder, G. F. et al. Galaxy morphology and star formation in the Illustris Simulation at $z=0$. *Mon. Not. R. Astron. Soc.* **454**, 1886–1908 (2015).
57. Rodriguez-Gomez, V. et al. The merger rate of galaxies in the Illustris simulation: a comparison with observations and semi-empirical models. *Mon. Not. R. Astron. Soc.* **449**, 49–64 (2015).
58. DeFelippis, D.et al. A Comparison of circumgalactic MgII absorption between the TNG50 simulation and the MEGAFLOW survey. Preprint at https://arxiv.org/abs/2102.08383 (2021).
59. Fuse, C., Marcum, P. & Fanelli, M. Extremely isolated early-type galaxies in the Sloan Digital Sky Survey. I. The sample. *Astron. J.* **144**, 57 (2012).
60. Genel, S. et al. The size evolution of star-forming and quenched galaxies in the IllustrisTNG simulation. *Mon. Not. R. Astron. Soc.* **474**, 3976–3996 (2018).
61. Benitez-Llambay, A. py-sphviewer: Py-SPHViewer v1.0.0 https://zenodo.org/record/21703#.YQK-zehKhaQ (2015).

Acknowledgements

J.A.B. and M.G.A. acknowledge financial support from CONICET through PIP grant 11220170100527CO. L.V.S. is grateful for support from NSF grant CAREER-1945310 and NASA grant ATP-80NSSC20K0566. A.P. acknowledges support from the Deutsche Forschungsgemeinschaft (DFG, German Research Foundation) through project 138713538 - SFB 881 ('The Milky Way System', subproject C09). D.N. acknowledges funding from the DFG through an Emmy Noether Research Group grant (NE 2441/1-1). F.M. acknowledges support through the programme 'Rita Levi Montalcini' of the Italian MUR. M.C. is partially supported by NSF grants AST-1518257 and AST-1815475. P.T. acknowledges support from NSF grants AST-1909933 and AST-200849 and from NASA ATP grant 80NSSC20K0502. M.V. acknowledges support from NASA ATP grants 16-ATP16-0167, 19-ATP19-0019, 19-ATP19-0020 and 19-ATP19-0167 and from NSF grants AST-1814053, AST-1814259, AST-1909831 and AST-2007355.

Author contributions

The listed authors made substantial contributions to this manuscript; all co-authors read and commented on the document. J.A.B. led the analysis of the simulation, compiled observational data from the literature and made all figures. L.V.S. and M.G.A. are responsible for the original idea and mentorship of J.A.B. throughout the project. L.V.S. led the writing of the manuscript and the response to the referee report with substantial contributions from J.A.B., M.G.A., A.P., D.N., F.M. and L.H. Co-author M.C. provided the expertise on the observational consequences of the results and on the study of quenching of dwarf galaxies. A.P., D.N., F.M., R.P., P.T., M.V. and L.H. are core members of the TNG50 simulation who set up, developed and ran the simulation that this manuscript is based on.

Competing interests

The authors declare no competing interests.

Additional information

Supplementary information The online version contains supplementary material available at https://doi.org/10.1038/s41550-021-01458-1.

Correspondence and requests for materials should be addressed to J.A.B.

Peer review information *Nature Astronomy* thanks Arianna Di Cintio and the other, anonymous, reviewer(s) for their contribution to the peer review of this work.

Reprints and permissions information is available at www.nature.com/reprints.

Publisher's note Springer Nature remains neutral with regard to jurisdictional claims in published maps and institutional affiliations.